Front. Chem. China 2009, 4(2): 136–141
DOI 10.1007/s11458-009-0023-x

RESEARCH ARTICLE

Yuanlin REN, Bowen CHENG, Jinshu ZHANG, Weimin KANG, Zhenhuan LI, Xupin ZHUANG

Study on thermal decomposition kinetics of *N*,*N*'-bis(5, 5-dimethyl-2-phospha-2-thio-1,3-dioxan-2-yl)ethylenediamine in air

Abstract The thermal decomposition kinetics of the *N*, *N*′-bis(5,5-dimethyl-2-phospha-2-thio-1,3-dioxan-2-yl) ethylenediamine (DPTDEDA) in air were studied by TG-DTG techniques. The kinetic parameters of the decomposition process for the title compound in the two main thermal decomposition steps were calculated through the Friedman and Flynn-Wall-Ozawsa (FWO) methods and the thermal decomposition mechanism of DPTDEDA was also studied with the Coats-Redfern and Achar methods. The results show that the activation energies for the two main thermal decomposition steps are 128.03 and 92.59 $kJ \cdot mol^{-1}$ with the Friedman method, and 138.75 and 106.78 $kJ \cdot mol^{-1}$ with the FWO method, respectively. Although there are two main thermal decomposition steps for DPTDEDA in air, the thermal decomposition mechanism of DPTDEDA in the two steps are the same, *i.e.* $f(\alpha) = 3/2(1-\alpha)^{4/3}[(1-\alpha)^{-1/3}-1]^{-1}$.

Keywords *N*, *N*′-bis(5, 5-dimethyl-2-phospha-2-thio-1, 3-dioxam-2-yl)ethylenediamine, thermal decomposition kinetics, activation energy, mechanism

1 Introduction

The fire retardants have been widely used for the materials which need to have flame retardance characteristics. In the recent years, the study on fire retardants has been spurred with the increasing worldwide flame retardance requirements. Fire retardants containing halogen (bromine or chlorine) have wide applications for their high fire retarded properties for the materials, but they can release toxic or corrosive hydrogen halide gases during the decomposition [1]. In particular, bromodiphenyl ether fire retardants can not only release toxic hydrogen bromide but also carcinogenic bromofuran during the thermal decomposition, which made the European Union, the United States and other countries or areas begin to restrict their applications [2, 3]. Thus, the research on fire retardants that are nearly non-toxic or those that do not release corrosive gases during decomposition greatly pushes the development of fire retardants containing non-halogen materials [4–8]. There are wide varieties of fire retardants containing phosphorus [9–11]. They can form phosphoric acid during thermal decomposition, which is a type of strong dehydrating agent. They can promote the fire retarded materials to dehydrate and char so as to form a layer of char residue on the surface of the fire retarded material, which can isolate the material from oxygen, so that fire retardance is achieved. The fire retardants containing nitrogen will not produce hydrogen halide and carcinogenic compounds as fire retardants containing halogen do. They have wide applications as fire retarded materials for their low smoke and environmentally friendly properties [2, 12, 13]. The new types of intumescent fire retardants are mainly composed of compounds containing phosphorus and nitrogen. They have rich acid source, carbon source and gas source, and are prospective fire retardants [14–17]. Some researches have shown that [18–21] sulfur is a kind of important fire retarded element, which has synergism with phosphorus and nitrogen. But there are few fire retardants which simultaneously contain phosphorus, sulfur and nitrogen in the same molecular structure. In the present work, TG-DTG techniques are applied to study the non-isothermal decomposition process in air of *N*,*N*′-bis(5,5-dimethyl-2-phospha-2-thio-1, 3- dioxan-2-yl)ethylenediamine (DPTDEDA) (as is shown in Scheme 1) which was synthesized by the authors of this manuscript, and the kinetics of DPTDEDA decomposition were analyzed by the Friedman method and Flynn-Wall-Ozawa (FWO) method. The kinetic parameters of the two

Translated from *Acta Chimica Sinica*, 2008, 66(9) (in Chinese)

Yuanlin REN (✉), Bowen CHENG, Jinshu ZHANG, Weimin KANG, Zhenhuan LI, Xupin ZHUANG
School of Textile of Tianjin Polytechnic University; Tianjin Municipal Key Laboratory of Fiber Modification and Functional Fiber, Tianjin Polytechnic University, Tianjin 300160, China
E-mail: yuanlinr@163.com

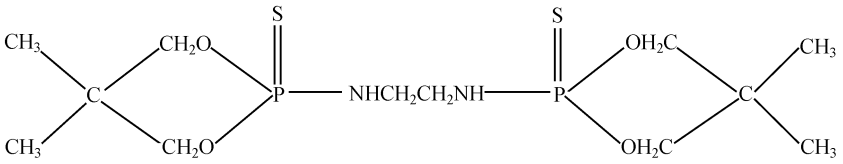

Scheme 1

main thermal decomposition stages were calculated, and the thermal degradation mechanism of DPTDEDA was studied with the Coats-Redfern method and Achar method.

2 Experiment

2.1 Synthesis and characterization of DPTDEDA

The synthesis of DPTDEDA was done according to Ref. [22], and DPTDEDA was recrystallized from a mixture with the same volume of acetone, anhydrous ethanol and water with its m.p. at 291–292°C. Elemental analysis gave: actual tested (calculated) /%, C:36.96(37.08), H:6.72 (6.70), P:15.75(15.97); FTIR(KBr pellet ν/cm^{-1}): 3350.2(νNH), 2972.52 (νCH$_3$), 1473.91(νCH$_2$), 1043.54, 986.6 (νP–O–C), 972.45 (νP–N), 683.24 (νP = S); ^{1}H–NMR(CDCl$_3$), δ: 0.91–0.92(m, 12H, exomethyl), 3.84–4.04(m, 4H, exomethylene), 4.23–4.30(m, 8H, ring methylene), 6.52(d, 2H, NH). MS m/z: 318(M$^+$).

2.2 Apparatus and test conditions

TG-DTG analysis for DPTDEDA was conducted on a NETZSCH STA 409 PG/PC Thermal Analyzer. The experiment was conducted under air at the flow rate of 20 mL/min and at various heating rates(5, 10, 15 and 20 K/min) from room temperature to 1000°C, and the sample weight was 4–5 mg.

2.3 Kinetic methods

As to the thermal decomposition reaction, the reaction rate can be usually expressed as:

$$\mathrm{d}\alpha/\mathrm{d}t = kf(\alpha) \tag{1}$$

According to Arrhenius equation, $k = A\mathrm{e}^{-E/RT}$, the following equation can be achieved.

$$\mathrm{d}\alpha/\mathrm{d}t = A\mathrm{e}^{-E/RT}f(\alpha) \tag{2}$$

where α is the decomposed mass fraction(%) at time t, A is the pre-exponential factor (s^{-1}), E is the apparent activation energy (kJ·mol^{-1}), R is the gas constant (J·mol^{-1}·K^{-1}), $f(\alpha)$ is the reaction mechanism function. Under the controlled and constant heating rate, the rate of temperature rising, *i.e.* $\beta = \mathrm{d}T/\mathrm{d}t$, thus, Eq. (2) can be changed to the follows:

$$\mathrm{d}\alpha/\mathrm{d}T = (A/\alpha)\mathrm{e}^{-E/RT}f(\alpha) \tag{3}$$

Through separating the variable and rearranging with the integral or differential functions of Eq. (3), the Friedman equation [23,24] and the Flynn-wall-Ozawa(FWO) equation [25,26] can be gained respectively as follows:

$$\ln[(\mathrm{d}\alpha/\mathrm{d}T)\beta] = \ln[Af(\alpha)] - E/RT \tag{4}$$

$$\lg\beta = \lg[AE/RG(\alpha)] - 2.315 - 0.4567E/RT \tag{5}$$

Logging the Eq. (3), the Coats-Redfern integral equation [27,28] and Achar differential equation [29] can be gained respectively as follows:

$$\ln[G(\alpha)/T^2] = \ln(AR/\beta E) - E/RT \tag{6}$$

$$\ln[(\mathrm{d}\alpha/\mathrm{d}T)/f(\alpha)] = \ln(A/\beta) - E/RT \tag{7}$$

According to Coats-Redfern equation and Achar equation, the authors selected the normal used thirty types kinetic functions $G(\alpha)$ and $f(\alpha)$ from Ref. [29], and plotted $\ln[G(\alpha)/T^2]$ and $\ln[(\mathrm{d}\alpha/\mathrm{d}T)/f(\alpha)]$ against $1/T$, the regression curves could be generated by the least square method, and the kinetic parameters E, $\ln A$ and correlation coefficient r of the different mechanism functions could be obtained.

3 Results and discussion

3.1 The thermal decomposition of DPTDEDA

The TG and DTG curves of DPTDEDA at different heating rates in air are shown in Fig. 1. The TG and DTG curves of DPTDEDA at the heating rates of 10 K/min in air are shown in Fig. 2. As shown in Fig. 1, with the increasing heating rates, the initial decomposition temperature (T_i), the mass loss peak temperature (T_p) and the decomposition termination temperature (T_d) of the DTG curves of DPTDEDA at the different four heating rates rise correspondingly. It can be seen that the DTG curves and TG curves shift toward the high temperature zone. This may be because the heating rates can affect the temperature gradient and heat transmission between the pot and sample, outside sample and inside sample. When the heating rates is slow, the sample can have enough time to expose to specific temperature to absorb heat, which makes

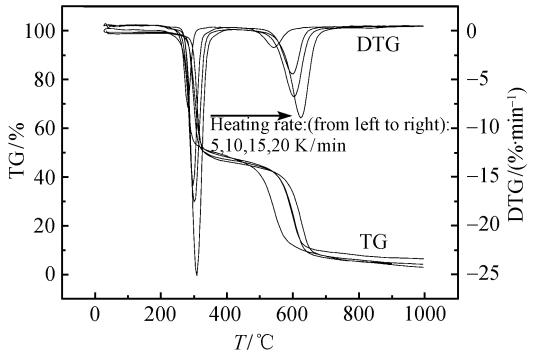

Fig. 1 TG-DTG curves of DPTDEDA at heating rates of 5,10,15,20 K/min in air

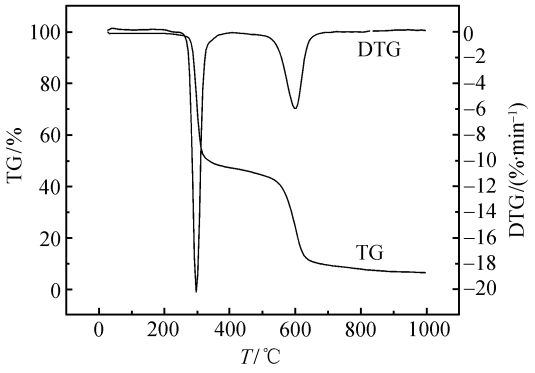

Fig. 2 TG-DTG curves of DPTDEDA at heating rate of 10 K/min in air

the initial decomposition temperature and the termination temperature lower. While with the increasing heating rates, the heat transmission rate slows down. The sample has not much time to accept heat supplied from the outer environment, which leads to higher temperature to supply heat to decompose [30]. In addition, as is shown in Fig. 1, the weight loss temperature range and the weight losing rates at the four heating rates are different, but the total weight losses are almost same when the sample is heated to the specific temperature (1000°C).

As shown in Fig. 2, the TG curve of DPTDEDA has two main weight loss stages. There is 49.66% mass loss in the first stage (267.9–377.2°C), and the temperature peak of the fastest weight loss is 281.2°C. There is a relative weak P = S double bond in the DPTDEDA structure [31,32]. In the presence of oxygen, sulfur removal reaction happens first in the first weight loss stage to produce SO_2. Then, the breaking of P–O bond and P–N bond occurs, and phosphorus forms phosphoric acid in this period followed by dehydration of phosphoric acid to form metaphosphoric acid. Then, it polymerizes to polymetaphosphoric acid which promotes neopentyl glycol to dehydrate and char. At the same time, DPTDEDA decomposes to release NH_3. There is 40.25% weight loss (506.6–667.1°C) in second stage, and the fastest weight loss temperature is 542.5°C. The weight loss of this stage is mainly due to the CO_2 release resulting from the carbon oxidization at higher temperature. The two weight loss stages are consistent with the decomposition temperature of the most polymers. There is over 25% char residue at 600°C, and 2.92% char residue left at the specific temperature (1000°C), which illustrates that DPTDEDA has good thermal stability and excellent char forming capability, and it can give excellent fire retardance for the condensation phase. There are two thermal decomposition peak in the DTG curve. The first one is narrow and sharp, which shows that the weight loss is very fast and this is consistent with the relative small temperature range of the first main weight loss of the TG curve. Compared with the first weight loss peak, the second peak is wide and passive, which shows that the weight loss is relative moderate, and this agrees with the relative wide weight loss temperature range of the second main weight loss stage of the TG curve.

3.2 Fire retardant properties

The tests on the fire retarded viscose with DPTDEDA fire retardant show that when the mass fraction of DPTDEDA in the viscose is 18% the limited oxygen index (LOI) values of the viscose can increase from 17% to over 28%. The SEM of the fire retarded viscose is shown in Fig. 3. It can be seen that the burned sample surface has many bulge bubbles, and the cross section of the sample is honeycomb like structure. It is because the SO_2 and NH_3 produced from the decomposition of DPTDEDA collide against the fire retarded system, which shows that DPTDEDA is an intumescent fire retardant.

3.3 Thermal decomposition kinetics

The Friedman method and Flynn-wall-Ozawa (FWO) method are the common methods to calculate the activation energy in the equal conversion rate method. As $\alpha < 0.1$ or $\alpha > 0.9$, the decomposition reaction is in induction or end period, which can not fully reflect the real state of the degradation, and may bring uncertainty to the judgment on the mechanism function. So, the conversion rate, α should be selected between 0.1–0.9. The α, T, $d\alpha/dt$ data of the thermal decomposition of DPTDEDA are listed in Table 1. Bring the corresponding experimental data obtained from the two main weight loss stages of the thermal decomposition of DPTDEDA in air into the Eqs. (4) and (5), and calculating the activation energy of the decomposition reaction with computer, then the E values correspond to different α are listed in Table 2. As shown in Table 2, the reaction activation energies calculated with FWO method are slightly higher than those values obtained from the Friedman method. The E values attained from Friedman method appear fluctuations with the increasing α, which is due to the Friedman equation being sensitive to noise signals. However, in the

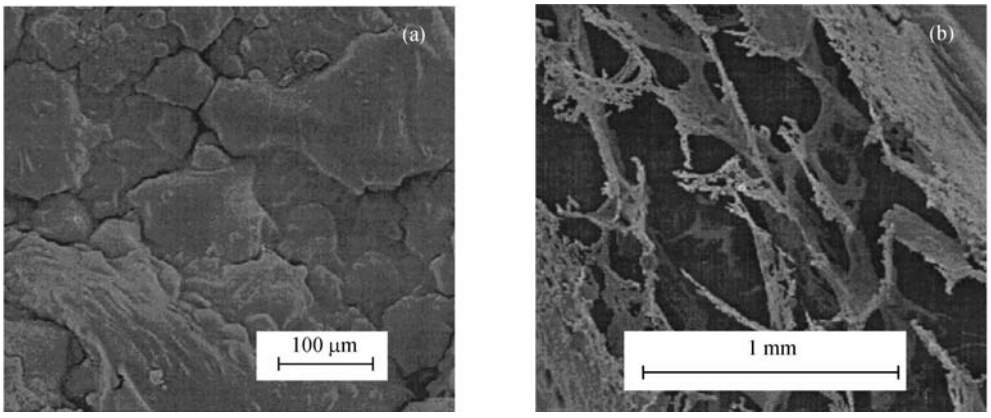

Fig. 3 SEM pictures of the char residue of fire retarded viscose
(a) SEM of the surface view of the char residue of fire retarded viscose; (b) SEM of the cross-section view of the char residue of fire retarded viscose

Table 1 Data of thermal decomposition of DPTDEDA from TG-DTG curves at different heating rates

α	β							
	5		10		15		20	
	T/K	dα/dt	T/K	dα/dt	T/K	dα/dt	T/K	dα/dt
0.10	543.60	4.36	562.28	12.1	563.58	13.81	573.00	22.15
0.15	548.18	6.69	565.58	14.90	567.91	16.67	576.31	24.83
0.20	550.97	7.94	568.38	16.48	571.21	18.17	579.11	26.22
0.25	553.77	8.61	571.18	17.06	574.86	18.73	581.39	26.63
0.30	558.17	8.34	573.97	16.54	578.25	18.26	583.51	26.40
0.35	541.70	7.35	576.77	14.94	581.97	17.04	585.80	25.76
0.40	564.11	4.78	580.33	12.04	586.38	14.24	588.60	23.92
0.45	571.74	3.68	585.16	7.60	592.14	9.52	592.92	20.10
0.60	779.79	1.02	797.80	2.34	807.63	4.67	860.60	4.77
0.65	797.58	1.83	849.82	3.58	851.55	5.08	868.85	5.71
0.70	809.45	2.27	861.94	4.70	863.75	6.72	883.26	8.40
0.75	821.31	2.25	871.26	5.15	873.67	7.54	89425	9.71
0.80	831.99	1.84	881.52	4.77	883.59	7.27	902.75	9.56
0.85	849.79	1.03	893.64	2.94	893.50	6.10	912.92	8.14

Table 2 The apparent activation energy values of DPTDEDA in the two thermogravimetric steps at the different conversions calculated by Friedman and Flynn-Walls-Ozawa methods respectively

The first thermogravimetric step			The second thermogravimetric step		
α/%	Friedman /(kJ·mol^{-1})	FWO /(kJ·mol^{-1})	α/%	Friedman /(kJ·mol^{-1})	FWO /(kJ·mol^{-1})
0.15	120.35	122.40	0.60	90.11	96.68
0.20	105.36	118.37	0.65	102.60	90.79
0.25	102.79	122.45	0.70	84.93	84.72
0.30	116.37	138.64	0.75	88.04	98.68
0.35	126.16	138.64	0.80	94.04	117.77
0.40	161.00	138.77	0.85	95.22	154.29
0.45	240.29	133.39	0.90	93.15	104.5
Mean	128.03	138.75	Mean	92.59	106.78

Table 3 The calculated values of kinetic parameters of the DPTDEDA in the first thermogravimetric step by Coats-Redfern method and Achar method respectively

Coats-Redfern method					Achar method				
β	E	lg A_S	R	SD	β	E	lg A_S	R	SD
5	126.14	11.37	−0.9986	0.0355	5	125.33	11.24	−0.9887	0.0545
10	129.24	11.43	−0.9984	0.0355	10	130.14	11.48	−0.9984	0.0360
15	130.16	11.51	−0.9928	0.0747	15	130.09	11.46	−0.9929	0.0738
20	124.76	11.12	−0.9994	0.0223	20	127.59	11.29	−0.9994	0.0210
Mean	127.58	11.36	−0.9973	0.0420	Mean	128.29	11.37	−0.9949	0.0463

Table 4 The calculated values of kinetic parameters of the DPTDEDA in the second thermogravimetric step by Coats-Redfern method and Achar method respectively

Coats-Redfern method					Achar method				
B	lg A_S	E	R	SD	β	E	lg A_S	R	SD
5	85.51	3.71	−0.9985	0.0141	5	90.13	3.62	−0.9939	0.0050
10	95.96	4.06	−0.9985	0.0147	10	100.23	4.29	−0.9985	0.0147
15	103.57	4.27	−0.9982	0.0131	15	97.25	3.96	−0.9932	0.0427
20	91.74	4.35	−0.9869	0.0425	20	89.77	4.39	−0.9869	0.0425
Mean	94.20	4.10	−0.9955	0.0211	Mean	94.35	4.06	−0.9931	0.0263

FWO method, the E values of the two main decomposition stages change little with the increasing α, which shows that the decomposition reaction represented by the respective two stages may be a one step reaction.

3.4 Mechanism speculation

According to the Coats-Redfern equation and Achar equation, the authors selected the normally used thirty types kinetic functions $G(\alpha)$ and $f(\alpha)$ from Ref. [29], and plotted $\ln[G(\alpha)/T^2]$ and $\ln[(\mathrm{d}\alpha/\mathrm{d}T)/f(\alpha)]$ against $1/T$. The regression curves could be generated by the least square method and the kinetic parameters E, $\ln A$ and correlation coefficient r of the different mechanism functions could be obtained. Comparing the kinetic parameters values of E and $\ln A$ calculated from differential and integral method, selecting the closest E and $\ln A$ values and the better coefficient r. The reaction model of the E values being nearly equal to those calculated from Friedman or FWO method is the kinetic model. In this work, the data tested from the heating rates of 5, 10, 15, 20 K/min are calculated, respectively, and the results are listed in Table 3 and Table 4. Thus, the mechanism function of the first reaction stage is $f(\alpha)= 3/2(1-\alpha)^{4/3}[(1-\alpha)^{-1/3}-1]^{-1}$. Taking the average values of differential and integral methods, the activation energy is $E = 127.93\ \mathrm{kJ\cdot mol^{-1}}$, and the pre-exponential factor is $\lg A = 11.36\ \mathrm{s^{-1}}$. While the mechanism function of the second stage is $f(\alpha)= 3/2(1-\alpha)^{4/3}[(1-\alpha)^{-1/3}-1]^{-1}$, activation energy is $94.27\ \mathrm{kJ\cdot mol^{-1}}$, and the pre-exponential factor is $\lg A = 4.08\ \mathrm{s^{-1}}$. Though there are two main thermal weight loss stages of DPTDEDA in air, the reaction mechanism function is the same one by calculating, *i.e.* $f(\alpha) = 3/2(1-\alpha)^{4/3}[(1-\alpha)^{-1/3}-1]^{-1}$.

References

1. Tange L, Drohmann D. Environmental issues related to end-of-life options of plastics containing brominated flame retardants. Fire and Materials, 2004, 28(5): 403–410
2. Lu S Y, Hamerton I. Recent developments in the chemistry of halogen[hyphen]free flame retardant polymers. Prog Polym Sci, 2002, 27(8): 1661–1712
3. Wu Y L, Wang C A, Xu K, Chen M C. Some aspect of preparation and application of halogen-free flame retardant polymers containing phosphorus. Polymer Bulletin, 2005, 6: 37–42, 83 (in Chinese)
4. Catala J M, Brossas J. Synthesis of fire-retardant polymers without halogens. Prog Org Coat, 1993, 22(1–4): 69–82
5. Davis J. The technology of halogen-free flame retardant additives for polymeric systems. Engineering Plastic, 1996, 9(5): 403–419
6. Grande J A. Halogen-free, flame-retardant TPU targets wire and cable, mass transit. Modern Plastics, 1998, 75(2): 95
7. Ng W. Flame-retardant suppliers shift to halogen-free grades. Modern Plastics, 1999, 76(10): 84
8. Morgan A B, Tour J M. Synthesis and Testing of Nonhalogenated Alkyne-Containing. Flame-Retarding Polymer Additives. Macromolecules, 1998, 31(9): 2857–2865
9. Weil E D, Levchik S V, Ravey M, Zhu W M. A survey of recent progress in phosphorus-based flame retardants and some mode of action studies. Phosphorus Sulfur Silicon Relat Elem, 1999, 146: 17–20
10. Woodward G, Harris C, Manku J. Design of new organophosphorus

flame retardants. Phosphorus Sulfur Silicon Relat Elem, 1999, 146: 25–28

11. Aaronson A M, Bright D A. Oligomeric phosphate esters as flame retardants. Phosphorus Sulfur Silicon Relat Elem, 1996, 110(1–4): 83–86
12. Horacek H, Grabner W. Nitrogen based flame retardants for nitrogen containing polymers. Makromol Chem Macromol Symp, 1993, 74: 271–276
13. Weil E, Mcswigan B. Melamine phosphates and pyrophosphates in flame-retardant products with new potential. J Coat Technol, 1994, 66(839): 75–82
14. Li Q, Jiang P K, Wei P. Synthesis, characteristic, and application of new flame retardant containing phosphorus, nitrogen, and silicon. Polym Eng Sci, 2006, 46(3): 344–350
15. Yang C Q, Wu W D, Xu Y. The combination of a hydroxy-functional organophosphorus oligomer and melamine-formaldehyde as a flame retarding finishing system for cotton. Fire and Materials, 2005, 29(2): 109–120
16. Abdel-Mohdy F A. Graft copolymerization of nitrogen- and phosphorus-containing monomers onto cellulosics for flame-retardant finishing of cotton textiles. J Appl Polym Sci, 2003, 89 (9): 2573–2579
17. Liu Y, Wang Q. Preparation of microencapsulated red phosphorus through melamine cyanurate self-assembly and its performance in flame retardant polyamide 6. Polym Eng Sci, 2006, 46(11):1548–1553
18. Karaivanova M, MihailovaN, GjurovaK. The effect of sulfur- and nitrogen-containing fire retardants on reducing the flammability of a polychloroprene composition used for cables. J Appl Polym Sci, 1990, 40(11–12): 1939–1949
19. Karaivanona M S, Gjurova K M. Non-halogen-containing flame-retardant ethylene-propylene copolymer compositions for cable insulation with nitrogen- and sulfur-containing fire retardants. J Appl Polym Sci, 1997, 63(5): 581–588
20. Koutu B B, Sharma R K. Synthesis of a flame-retardant dope additive dithiopyrophosphate and its effect on viscose rayon fibres. Indian J Fibre Text Res, 1996, 21: 140–142
21. Lewin M, Brozek J, Martens M M. POLYMERS FOR ADVANCED TECHNOLOGIES. Polym Adv Tech, 2002, 13(10–12): 1091–1102
22. Cheng B W, Ren Y L. Synthesis of a kind of cellulose fire retardant. CN 1563160, 2004 (in Chinese)
23. Tao Y T, Zhan D, Zhang KL. Acta Chim Sinica, 2006, 64(5): 435–438 (in Chinese)
24. Friedman H L. Kinetics of thermal degradation of charforming plastics from thermogravimetry. Application to a phenolic plastic. J Polym Sci, Part C, 1964, 6(1):183–195
25. Chen P, Zhao F Q, Luo Y, Hu R Z, Zheng Y M, Deng M Z, Gao Y. Acta Chim Sinica, 2004, 62(13): 1197–1204 (in Chinese)
26. Ozawa T. A new method of analyzing thermogravimetric data. Bul1 Chem Soc Jpn, 1965, 38: 1881–1886
27. Coats A W, Redfern J P. Kinetic parameters from thermogravimetric data. Nature, 1964, 201(1): 68–69
28. Xing Y H, Yuan H Q, Zhang Y H, Zhang B L, Xu F, Sun L X, Niu S Y, Bai F Y. Chem J Chinese Universities, 2006, 27(7): 1205–1210 (in Chinese)
29. Hu R Z, Shi Q Z. Thermal Analysis Kinetics. Beijing: Science Press. 2001, 65 (in Chinese)
30. Li S H, Bai J R, Sun B Z, Hu A J, Wang Q. Effect of heating rate on the pyrolysis characteristics of oil shales. Chemical Engineering, 2007, 35(1): 64–67 (in Chinese)
31. Luo Y R. Handbook of Chemical Bond Dissociation Energies Data. Beijing: Science Press. 2005, 295
32. Dean J A. Lange's Handbook of Chemistry. 15 edn. New York: McGraw-Hill, Inc. 1999, 587–594